

Experimental and computational studies on doped-Ag₂O photocatalysts



Thesis submitted in partial fulfillment

for the Award of Degree

Doctor of Philosophy

by

ARUP KUMAR DE

**DEPARTMENT OF CHEMISTRY
INDIAN INSTITUTE OF TECHNOLOGY
(BANARAS HINDU UNIVERSITY)
VARANASI- 221005**

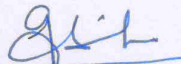
Roll No. 17051015

Year. 2022

CERTIFICATE

It is certified that the work contained in the thesis titled "*Experimental and computational studies on doped-Ag₂O photocatalysts*" by "*Arup Kumar De*" has been carried out under my supervision and this work has not been submitted elsewhere for a degree.

It is further certified that the student has fulfilled all the requirements of Comprehensive, Candidacy and SOTA for the award of Ph.D Degree.


Dr. Indrajit Sinha
(Supervisor)

Department of Chemistry
Indian Institute of Technology
(Banaras Hindu University)

DECLARATION BY THE CANDIDATE

I, "Arup Kumar De", certify that the work embodied in this thesis is my own bona fide work and carried out by me under the supervision of "Dr. Indrajit Sinha" from "July 2017" to "July 2022", at the "Department of Chemistry", Indian Institute of Technology (BHU), Varanasi. The matter embodied in this thesis has not been submitted for the award of any other degree/diploma. I declare that I have faithfully acknowledged and given credits to the research workers wherever their works have been cited in my work in this thesis. I further declare that I have not willfully copied any other's work, paragraphs, text, data, results, etc., reported in journals, books, magazines, reports dissertations, theses, etc., or available at websites and have not included them in this thesis and have not cited as my own work.

Date: 20.07.2022

Place: Varanasi

Arup Kumar De

Signature of the Student

(Arup Kumar De)

CERTIFICATE BY THE SUPERVISOR

It is certified that the above statement made by the student is correct to the best of my knowledge.

Dr. Indrajit Sinha. 21/7/22
(Supervisor)

Department of Chemistry
Indian Institute of Technology
(Banaras Hindu University)


Signature of Head of Department

विभागाध्यक्ष / HEAD
रसायन विज्ञान विभाग
Department of Chemistry
भारतीय प्रौद्योगिकी संस्थान (का.हि.वि.वि.)
Indian Institute of Technology (B.H.U.)
वाराणसी-221005 / Varanasi-221005

COPYRIGHT TRANSFER CERTIFICATE

Title of the Thesis: *“Experimental and computational studies on doped-Ag₂O photocatalysts”*

Name of the Student: Arup Kumar De

Copyright Transfer

The undersigned hereby assigns to the Indian Institute of Technology (Banaras Hindu University) Varanasi all rights under copyright that may exist in and for the above thesis submitted for the award of the *“Ph.D. Degree”*.

Date: 21/07/2022

Place: Varanasi

Arup Kumar De
Signature of the Student

(Arup Kumar De)

Note: However, the author may reproduce or authorize others to reproduce material extracted verbatim from the thesis or derivative of the thesis for author's personal use provided that the source and the Institute's copyright notice are indicated.

ACKNOWLEDGEMENTS

I would like to acknowledge all who have directly or indirectly contributed through their invaluable support by conveying their experience, knowledge, encouragement and kindness during my research work. I believe that it would be very tough to achieve my goal.

*Firstly, I would like to express overwhelming gratitude to my supervisor, **Dr. Indrajit Sinha**, for his continuous encouragement and motivation throughout my research journey. He always used to maintain a peaceful environment in the Lab. His knowledge and expertise in the subject led to a thoughtful discussion of the research outcome. I am very thankful for his constant guidance and assistance in improving my writing skill in scientific journals and the genesis of research ideas. This will help the future aspect of my research carrier.*

*I would like to thank my RPEC members (internal), **Dr. Vikas Jindal**, Department of Metallurgical Engineering, former **Prof. R. B. Rastogi**, Department of Chemistry, and **Prof. D. Tiwari**, Department of Chemistry, for their kind suggestions during my research progress.*

*I express deep gratitude to the successive Heads of the Department of Chemistry of IIT (BHU), **Prof. R.B. Rastogi**, **Prof. D. Tiwari**, and **Prof. Y.C. Sharma** for all the support from the Department.*

I am thankful to all the faculty members of the Department of Chemistry of IIT (BHU) for their cooperation.

I want to acknowledge all the members of the Central Instrument Facility (CIF) of the institute for availing of the characterization facilities. I also thank the Central Discovery Centre (CDC) of BHU for the PL characterization.

I am grateful to Prof. Manoj Kumar, Department of Chemical Engineering, for availing me of his lab facility during my research work.

I am highly grateful to my senior lab mates, Dr. Alkadevi Verma, Dr. Sunil Kumar, Dr. Shaili Pal, and Dr. Jyoti Kuntail for their active discussions and valuable suggestions for any problems faced during the research activities.

I express my deepest thanks to my junior lab-mates, Neha Jataw, Neha Kamal, Anshu Shrivastava, Uttam Kumar, and Nivedita Singh for their presence and company made the journey joyful.

I am also thankful to Sourav Majumdar for his valuable co-operation.

I would also like to acknowledge MHRD, Govt. of India, for providing me with financial support for my research work and travel grants.

I would like to acknowledge Central Instrumentation Facility (CIF), IIT (BHU) for characterization and also acknowledge Dr. Roshan Singh &

other staff of the Centre for Computing and Information Services (CCIS), IIT (BHU) for their services.

*I am forever indebted to my father, **Anup Kumar De**, mother, **Bani De** and wife, **Jaya Roy**, for giving me the supports that have made me who I am. I praise and thank GOD, who has granted me countless blessings and opportunities.*

Table of Contents

Description	Page No.
List of Figures	xiii
List of Tables.....	xix
Symbols Used	xxi
Preface	xxiii
1. CHAPTER 1: Introduction and literature survey	1
1.1 Introduction	1
1.2 Composite photocatalysts	3
1.2.1 p-n heterojunction photocatalyst.....	4
1.2.2 Z-scheme photocatalysis.....	5
1.3 Importance of doping and defects in heterogeneous photocatalysis.....	6
1.4 Synthesis protocol of doped photocatalysts	8
1.4.1 Coprecipitation followed by calcination method.....	8
1.4.2 Sol-gel method.....	9
1.4.3 Reverse micelle method.....	9
1.4.4 Solvothermal or hydrothermal method	10
1.5 Synthesis of composites with doped photocatalysts	10
1.6 Computational approaches to the doped photocatalysts	11
1.7 Research gap	13

1.8	Objectives of the thesis	15
2.	CHAPTER 2: Materials and methods	17
2.1	Introduction.....	17
2.2	Chemicals	17
2.3	Sample preparation	19
2.4	Materials characterization techniques.....	19
2.4.1	Powder X-Ray Diffraction (XRD)	20
2.4.2	Transmission Electron Microscopy (TEM) sample preparation and imaging	21
2.4.3	Scanning Electron Microscope (SEM) sample preparation and imaging	22
2.4.4	UV-Visible spectroscopy	23
2.4.5	UV-visible diffuse reflectance spectroscopy (UV- DRS)	24
2.4.6	X-ray photoelectron spectroscopy (XPS).....	25
2.4.7	Spectrofluorimetry.....	26
2.5	Photocatalytic performance measurements	27
2.6	Electrochemical measurements	28
2.7	Computational protocol	29
2.7.1	Plane-wave density functional theory (DFT)	29
2.7.2	Computational protocol.....	30
3.	CHAPTER 3: Zn doped Ag₂O photocatalysts.....	31
3.1	Introduction.....	31
3.2	Experimental.....	33

3.2.1	Sample Preparation	33
3.2.2	Computational Details	34
3.2.3	Photocatalytic Performance Measurements	36
3.3	Results and Discussion.....	37
3.3.1	Structural Properties	37
3.3.2	DFT calculations.....	41
3.3.3	TEM analysis	45
3.3.4	XPS analysis	47
3.3.5	Bandgap analysis	49
3.3.6	Fluorescence spectra	50
3.3.7	Photocatalytic activity.....	51
3.4	Conclusions	59
4.	CHAPTER 4: Ni doped Ag₂O photocatalysts	61
4.1	Introduction	61
4.2	Experimental Section	64
4.2.1	Sample preparation	64
4.2.2	DFT calculations.....	65
4.2.3	Photocatalytic activity measurements.....	66
4.3	Result and discussion	67
4.3.1	Structural Properties:	67
4.3.2	XPS analysis	72
4.3.3	Photoluminescence Study	79

4.3.4	DFT calculations	80
4.3.5	Photocatalytic efficiency assessment	82
4.3.6	Proposed mechanism.....	85
4.4	Conclusions.....	86
5.	CHAPTER 5: S doped Ag₂O photocatalysts	88
5.1	Introduction.....	88
5.2	Experimental.....	91
5.2.1	Sample preparation.....	91
5.2.2	Computational details.....	92
5.2.3	Photocatalysis experimental details.....	94
5.3	Results and discussion	95
5.3.1	Structural properties	95
5.3.2	TEM and SEM analysis.....	97
5.3.3	The bandgap	99
5.3.4	Photoluminescence studies.....	100
5.3.5	XPS analysis.....	101
5.3.6	DFT calculation results	105
5.3.7	Photocatalytic properties	110
5.3.8	Plausible photocatalytic mechanism	113
5.4	Conclusions.....	115
6.	CHAPTER 6: Cd doped Ag₂O/BiVO₄ photocatalysts	116
6.1	Introduction.....	116

6.2	Experimental	118
6.2.1	Sample preparation	118
6.2.2	Computational methods	120
6.2.3	Photocatalytic experiment details	121
6.3	Results and discussion	122
6.3.1	Structural properties.....	122
6.3.2	XPS analysis	125
6.3.3	The bandgap.....	129
6.3.4	Electrochemical studies	130
6.3.5	DFT results	131
6.3.6	Photocatalytic properties.....	132
6.3.7	Plausible mechanism.....	136
6.4	Conclusions	137
7.	CHAPTER 7: Summary and conclusions	139
7.1	Summary	139
7.2	Future scope of the thesis work.....	143
8.	References	144

List of Figures

Description	Page No.
Figure 1.1 Schematic diagram of the single-phase semiconductor photocatalysis.....	3
Figure 1.2 The photocatalytic mechanisms followed in (a) p-n heterojunction, (b) Z scheme with staggered band alignment.	4
Figure 1.3 Schematic presentation of the effect of doping on photocatalysis.	6
Figure 1.4 A typical DOS plot of a semiconductor material.	13
Figure 2.1 Schematic diagram of Bragg's diffraction law.	21
Figure 2.2 TEM instrument (Model: Tecnai G2 20 TWIN).	22
Figure 2.3 FE-SEM instrument (model: Nano Nova SEM 450)	23
Figure 2.4 Agilent Cary 60 spectrophotometer.....	24
Figure 2.5 Shimadzu UV 2600 spectrophotometer.....	25
Figure 2.6 XPS instrument K-ALPHA model.	26
Figure 2.7 (a) Outer, and (b) inner view of the photocatalytic chamber.	27
Figure 3.1 Optimized supercells of (a) Ag ₂ O, (b) Ag ₂ O with Zn substituting an Ag, and (c) Ag ₂ O with Zn placed in an interstitial position.	35
Figure 3.2 (a) Normalized HR-XRD patterns of pure Ag ₂ O (A0) and different Zn doped Ag ₂ O (A1, A2, A3) samples (b) Comparison of the Ag ₂ O (111) peaks with the increase in Zn doping (from the HR-XRD patterns).	37
Figure 3.3 High-resolution XRD spectra of A4 (10 mol% Zn doping).	38
Figure 3.4 SEM images and corresponding EDS spectra of A1 (a, b), A2 (c, d), A3 (e, f) samples.	39
Figure 3.5 Variation in lattice parameter with Zn percentage.	40
Figure 3.6 The density of states plots for (a) pure Ag ₂ O and (b) Zn doped Ag ₂ O.	42

Figure 3.7 Partial density of states (PDOS) of (a) pure Ag ₂ O and (b) Zn doped Ag ₂ O.	44
Figure 3.8 Band structures of (a) pure Ag ₂ O and (b) Zn doped Ag ₂ O.	45
Figure 3.9 TEM analysis of A0.	46
Figure 3.10 TEM images of Zn doped Ag ₂ O samples a) A1, c) A2, and e) A3. Part b), d), and f) present the particle size distributions corresponding to samples A1, A2, and A3, respectively.	46
Figure 3.11 High resolution deconvoluted XPS spectra for (a,b) Ag 3d (samples A0 and A3) and (c,d) O1s (samples A0 and A3).	48
Figure 3.12 (a) UV-Visible absorption spectra and (b) Tauc plots of prepared samples A0, A1, A2, and A3.	49
Figure 3.13 Photoluminescence spectra of samples A0, A1, A2, and A3.	51
Figure 3.14 (a) Photocatalytic MO degradation of A3 (b) Comparison of photocatalytic performance of the different photocatalysts (c) Recyclability of A3 (d) Result of active species trapping experiments for A3 catalyst in the presence of various scavenger molecules.	52
Figure 3.15 Change in the UV-visible spectrum of RhB (showing its degradation) on visible light irradiation with time in the presence of the A3 photocatalyst sample.	53
Figure 3.16 UV-visible of an aqueous solution of MO under cool white LED visible light irradiation (without photocatalyst). In the absence of a photocatalyst, there is no change in the intensity of the MO UV-visible absorbance under the light.	54
Figure 3.17 Degradation of MO at different pH in the presence of A3 photocatalyst.	55
Figure 3.18 RhB degradation kinetic plots for sample catalysts (A0, A1, A2, and A3).	56
Figure 3.19 Schematic diagram of the proposed mechanism during photocatalysis.	58

Figure 4.1 (a) The X-ray diffraction patterns of N0, N1, and N2 samples, (b) The HR-XRDs of the region around the Ag ₂ O (111) peak for N0, N1, and N2 samples, (c) Lattice parameter change with dopant concentration.	68
Figure 4.2 Powder XRD patterns of N3 sample.	69
Figure 4.3 (a) A TEM image and (b) particle size distribution curve of N2 sample.	70
Figure 4.4 A TEM micrograph and particle size distribution of N0 sample.	71
Figure 4.5 The EDS spectrum and a SEM image of N2.	71
Figure 4.6 XPS survey spectrum of (a) N0, (b) N1, and (c) N2 samples.	72
Figure 4.7 Ag 3d deconvolution of (a) N0 and (b) N2 catalysts.	74
Figure 4.8 (a) O 1s peak deconvolution of the N0 sample (b) O 1s peak deconvolution of the N2 sample (c) the XPS valence band spectra of N0 and N2 sample.	76
Figure 4.9 Deconvoluted XPS spectra of Ni 2p for N2 sample.	77
Figure 4.10 (a) UV-Vis reflectance and (b) UV-Vis absorbance spectra of N0, N1, and N2.	77
Figure 4.11 The Tauc plots of samples N0, N1, and N2.	78
Figure 4.12 PL spectra of N0 and N2 samples.	79
Figure 4.13 (a) A comparison of the total density of states (TDOS) of the pure Ag ₂ O and OV-rich Ag ₂ O (b) Comparison of the total density of states (TDOS) of OV-rich Ag ₂ O and Ni doping.	81
Figure 4.14 (a) UV-Vis absorption spectra of photocatalytic degradation of CIP with undoped (N0) and doped catalysts (N1 and N2) (b) The variation of $-\ln(C/C_0)$ as a function of irradiation time (c) Trapping experiments for CIP degradation on N2 photocatalyst (d) reusability plot of N2 photocatalyst.	84
Figure 4.15 Schematic of the proposed CIP photo-degradation mechanism.	85
Figure 5.1 Optimized geometry of C0, C1, and C2 models.	94

Figure 5.2 (a) Powder XRD patterns of the undoped and S-doped Ag ₂ O samples, (b) A comparison of the B0, B1, and B2 Ag ₂ O (200) plane XRD reflections (zoomed-in Ag ₂ O (200) peak).	95
Figure 5.3 Powder XRD pattern of B3 sample.....	96
Figure 5.4 TEM images of B0 (a), B1 (c), B2 (e) and the particle size distribution of B0 (b), B1 (d), B2 (f).	97
Figure 5.5 High-resolution SEM micrographs of (a) B1 and (b) B2 samples.....	99
Figure 5.6 (a) The solid-state UV-visible absorption spectra and (b) Tauc plots of B0, B1, and B2 samples.	100
Figure 5.7 A comparison of the PL spectrum of B0, B1, and B2 samples.....	101
Figure 5.8 XPS survey spectrum of (a) B0 and (b) B2 samples.....	101
Figure 5.9 High resolution XPS spectrum of O 1s for (a) B0 and (b) B2 samples (c) high resolution XPS spectrum of S 2p for B2 sample.....	103
Figure 5.10 Comparison of high-resolution XPS spectrum of Ag 3d for undoped (B0) and doped (B2) Ag ₂ O.	104
Figure 5.11 Valence band XPS spectrum of B0 and B2 samples.	105
Figure 5.12 Band structure of (a) OV Ag ₂ O (C1 model), (b) OV Ag ₂ O with substitutional S doping (C2 model).....	107
Figure 5.13 Comparison of TDOS of OV Ag ₂ O (C1 model) and S doped Ag ₂ O system (C2 model).....	108
Figure 5.14 The TDOS and PDOS for OV Ag ₂ O with substitutional S doping system (C2 model).....	109
Figure 5.15 Comparison of PDOS of the dopant's atomic orbitals.....	110

Figure 5.16 (a) Plots of RhB degradation with irradiation time, (b) kinetics plots – $\ln(C/C_0)$ vs. t over different photocatalysts, (c) results of scavenging experiments with on the B2 photocatalyst catalyst, and (d) recyclability tests of the B2 photocatalyst...	111
Figure 5.17 UV-Vis absorbance plot of RhB degradation on (a) B0 and (b) B2 photocatalysts.....	112
Figure 5.18 Possible RhB degradation photocatalytic mechanism.....	114
Figure 6.1 (a) The powder XRD patterns of undoped (D0) and doped samples (D1 and D2) (b) the zoomed-in Ag_2O (111) peak part.	122
Figure 6.2 Powder XRD pattern of D3 sample.....	123
Figure 6.3 Comparison of powder XRD pattern of BiVO_4 nanoparticles and composite samples (D1/5V, D1/10V, D1/20V).	124
Figure 6.4 (a) TEM and (b) HRTEM images of the D1/10V sample.	125
Figure 6.5 Comparison of high-resolution $\text{Ag}3d$ spectra of D0 and D1 samples.....	126
Figure 6.6 XPS survey spectrum of D1/10V sample.....	127
Figure 6.7 (a) $\text{Ag} 3d$ comparison of D1 and D1/10V (b) $\text{Bi} 4f$ comparison of V0 and D1/10V, the valence band XPS of (c) D1, and (d) V0.	128
Figure 6.8 (a) UV-visible absorption spectrum of D1 and V0 samples. The Tauc plot of (b) D1 and (c) V0.....	129
Figure 6.9 (a) Nyquist plots for D1, V0, and D1/10V (b) Mott-Schottky plot of D1..	130
Figure 6.10 DFT calculation of (a) H_2O interaction with the Cd-doped Ag_2O (200) surface and (b) O_2 interaction with BiVO_4 surface.....	131
Figure 6.11 (a) Comparison of CIP photodegradation for composites samples with component catalyst (b) kinetics plot comparison (c) scavenger experiment on D1/10V catalyst (d) catalytic recyclability for D1 and D1/10V catalysts.	134

Figure 6.12 UV-Vis absorbance spectra of CIP degradation on D1/10V photocatalyst
(a) MeCN solvent (b) MeCN solvent along with O₂ purging. 135

Figure 6.13 A schematic of the mechanism proposed based on the experimental and
DFT calculation results. 137

List of Tables

Description	Page No.
Table 2.1 Details of chemicals used in this thesis.....	17
Table 3.1 Calculation of energy per atom with the variation supercell size of Ag ₂ O....	36
Table 3.2 Lattice parameter values found from XRD patterns.	40
Table 3.3 The change in supercell dimensions with Zn in an interstitial position.....	41
Table 3.4 Comparison of band gap of the synthesized samples by different methods ..	50
Table 3.5 A comparison of turnover frequencies (TOF) of MO on the prepared doped Ag ₂ O photocatalysts.	56
Table 3.6 A comparison of turnover frequencies (TOF) of the visible light aerobic degradation of RhB on the prepared doped Ag ₂ O photocatalysts.	57
Table 4.1 Elemental analysis of the N0, N1, and N2 samples using XPS.....	73
Table 4.2 The Ag ⁰ and Ag ¹⁺ percentage from the deconvolution of Ag 3d for the N0 and N2 catalyst samples.....	75
Table 4.3 Turn over frequency values of the un-doped and doped catalysts.....	83
Table 5.1 Variation in lattice parameter and average particle size with dopant concentration.....	98
Table 5.2 The position of VB and CB for the undoped and doped samples.....	105
Table 5.3 The formation energies and bandgap values of all the models attempted from DFT analysis.....	106
Table 5.4 Change of the lattice parameters on the increment of OV in Ag ₂ O lattice..	107
Table 5.5 Turn over frequency (TOF) and rate constant of B0, B1, and B2 catalysts for the photo-degradation of RhB.....	113

Table 6.1 Adsorption energies and interatomic distances for adsorption of H ₂ O and O ₂ on considered Cd-doped Ag ₂ O and BiVO ₄ surfaces.	132
Table 6.2 Turnover frequency (TOF) and rate constant of synthesized catalysts for the photo-degradation of CIP.	134
Table 7.1 Comparison of TOF values of differently doped photocatalysts (reported in the literature) with Zn-doped Ag ₂ O on MO degradation.	139
Table 7.2 Comparison of CIP degradation TOF values of doped photocatalysts (reported) with those prepared in this thesis.	141
Table 7.3 Compares TOF of differently doped photocatalysts (reported in literature) for RhB degradation with the Zn-doped and S-doped Ag ₂ O photocatalysts prepared in this thesis.	142

Symbols Used

E_g	Bandgap
VB	Valence band
CB	Conduction band
h^+	Holes
e^-	Electrons
$\cdot OH$	Hydroxyl Radical
NaOH	Sodium Hydroxide
$O_2^{\cdot -}$	Superoxide Radical
OVs	Oxygen vacancies
UV-DRS	Ultraviolet Visible Diffuse Reflectance Spectroscopy
XRD	X-ray Diffraction
TEM	Transmission Electron Microscopy
XPS	X-ray photoelectron spectroscopy
SEM	Scanning Electron Microscopy
W	Watt
λ	Lambda
Å	Angstrom
θ	Theta
MO	Methyl orange
RhB	Rhodamine B
CIP	Ciprofloxacin
k_{app}	Apparent rate constant

TOF	Turnover frequency
IPA	Isopropyl alcohol
KI	Potassium iodide
HOMO	Highest occupied molecular orbital
LUMO	Lowest unoccupied molecular orbital
UV-Vis	Ultraviolet-visible
t	Time
α	Absorption coefficient
DDDW	Deionized double distilled water
LED	Light emitting diode

Preface

Photocatalysis is a green and economical technique for wastewater treatment (organic pollutants degradation). A semiconductor photocatalyst absorbs photon energy when it is exposed to light. The absorbed energy excites the material's electrons from valence band (VB) to the conduction band (CB). Therefore, generating a substantial amount of holes (h^+) and electrons (e^-) makes the material capable of performing various oxidation and reduction reactions, respectively. An extensive literature survey reveals little research on developing doped small bandgap photocatalysts and their heterostructures with other semiconductors.

In this context, Ag_2O is a widely used photocatalyst with a bandgap range of 1.2-1.5 eV. Although it has a narrow bandgap giving an advantage of absorbing the maximum portion (UV and Visible) of the solar spectrum, it faces several issues. For instance, the narrow bandgap restricts its redox ability. Other significant issues are the photo-stability of the material and the recombination of photo-generated charge carriers (h^+ and e^-). Essentially, proper charge separation in the materials can reduce these problems. Doping of Ag_2O or its composite with other visible range bandgap semiconductors can give efficient photocatalysts. There are many reports on the construction of heterostructures with Ag_2O as one of the components. For instance, Ag/Ag_2O /reduced TiO_2 , Ag_2O/WO_3 , Curcumin/ Ag/Ag_2O , Ag_2O/Ag_3PO_4 , Ag_2O/Bi_2O_3 , etc., have been synthesized and found to possess efficient photocatalytic activities towards certain organic pollutants.

Before this thesis, only one report, on preparing Sr-doped Ag_2O nanostructures for photocatalytic degradation of organic pollutants, was available in the literature on

doped Ag₂O. Few computational investigations (plane-wave DFT calculations) also reported on Ag₂O and oxygen vacancies in Ag₂O. Structural and band structures can be collected from the DFT studies. Before this thesis, no plane-wave DFT investigations have been reported on doped Ag₂O nanomaterials in the literature. The limited knowledge of doped-Ag₂O photocatalysts inspired the present investigations.

This thesis investigates the effects of cation and anion doping on the photocatalytic properties of Ag₂O. Furthermore, an efficient heterostructure with a doped Ag₂O system has also been prepared. A simple hydrothermal protocol was followed for preparing photocatalysts investigated in this thesis. The hydrothermal protocol introduced oxygen vacancies in the prepared Ag₂O nanoparticles. Different characterization techniques, like XRD, UV-DRS, TEM, SEM, XPS, etc., were applied to characterize the synthesized photocatalysts. XRD, EDS (SEM or TEM), and DFT calculations were used to analyze the doping phenomena. The DFT calculations, along with XRD data, on formation energies revealed the position of the dopant atom in the Ag₂O crystal structure. The XPS characterization found the elements, their oxidation states, oxygen vacancies, and the VB edge of the photocatalyst. Then, the photocatalytic performances of these photocatalysts were evaluated towards particular organic pollutant degradation. Hence, the thesis seeks to investigate the doping of Ag₂O both experimentally and through computational investigations.

Chapter 1 of this thesis highlights the basics of the subject area (photocatalysis). An extensive literature survey is performed to find out the lacuna of the research. There are several issues involved in the photocatalytic material. Therefore, designing an efficient photocatalyst has become very important. It has been found that doping can be an efficient strategy to encounter those issues. Introducing cationic and

anionic dopants in pure Ag₂O is hardly reported. The main objectives of the thesis have been clearly discussed at the end of the chapter.

Chapter 2 details all the chemicals used for the sample preparation. The sample preparation protocol is also mentioned. The instrumentations involved in the present investigations are discussed in a proper manner. The design of the photocatalytic experiment and computational investigation are given at the end.

Chapter 3 focuses on the 1st objective of the thesis. The Zn doped Ag₂O is prepared to understand how the dopant affects the nanoparticle's lattice structure. When dopant is introduced into the lattice structure, there is a vital question of whether it will occupy a substitutional or interstitial position. A proper XRD analysis confirmed interstitial doping formation. A parallel DFT investigation supported this evidence. Further, experimental and qualitative DFT calculations demonstrated the bandgap widening phenomenon in the material. The Zn doping widened the bandgap up to 1.65 eV. The density of states (DOS) calculation gave the reason for the bandgap widening. The dopant mainly extends and shifts the valence band (VB) region, introducing the dopant's energy states. The Zn doping also improved the photocatalytic performance of the Ag₂O nanoparticles towards organic pollutant (methyl orange and rhodamine-B) degradation.

Chapter 4 deals with the second objective on incorporating Ni dopant in Ag₂O nanoparticles. This doping also affects the nanoparticle's lattice structure and bandgap. The material's bandgap decreased slightly due to the doping. The XRD and DFT results showed that Ni substitutes Ag in the Ag₂O lattice structure. Ni doping shifts the VB edge to a lower energy region. The XPS investigation highlights a synergistic effect of doping and oxygen vacancy defects in photocatalytic performance. Hence, the Ni-doped

Ag₂O nanoparticles showed an improved photocatalytic activity towards ciprofloxacin degradation.

Chapter 5 involves the preparation and characterization of sulfur (S) doped Ag₂O nanoparticles. Initial DFT calculations demonstrated oxygen substituted by sulfur in Ag₂O lattice could result in bandgap widening. This result inspired the preparation of S-doped Ag₂O nanoparticles. Experimentally, the bandgap widens up to 1.89 eV. XPS analysis revealed S doping increases the oxygen vacancy defects proportion. The VB edge shifted to a higher energy region due to doping. Extensive DFT calculations were undertaken to investigate the most stable sulfur dopant position in the Ag₂O crystal structure. Furthermore, DFT calculations also showed the qualitative effect of such crystal structure on the doped Ag₂O band structure. Eventually, the S-doped Ag₂O nanoparticles showed an enhanced visible light photocatalytic activity towards rhodamine-B degradation.

Chapter 6 of the thesis investigated the efficacy of a composite prepared with Cd doped Ag₂O nanoparticles. First, different Cd doped Ag₂O systems were synthesized by a hydrothermal protocol. A particular Cd-doped Ag₂O system was selected by XRD and DFT analysis. Next, the selected Cd doped Ag₂O system and BiVO₄ (another visible light photocatalyst previously prepared by a well-established protocol) were joined together by a similar hydrothermal technique. The generated heterostructure gave better efficiency and appropriate recyclability for photocatalytic ciprofloxacin degradation. The increased efficiency was due to its Z scheme electron transfer mechanism, which was proved by XPS analysis. DFT calculations showed that H₂O adsorbed and activated on the Cd-doped Ag₂O part, while O₂ interacted better with the BiVO₄ surface. This investigation and the scavenger experiment results helped elucidate the appropriate photocatalytic mechanism.

Chapter 7 is the last chapter of the thesis, which ends with a summary of all investigations and the future scope of these studies. These prepared photocatalysts' turnover frequency (TOF) values have been compared with those in the existing literature.

